SLOVAK UNIVERSITY OF TECHNOLOGY IN BRATISLAVA
FACULTY OF ELECTRICAL ENGINEERING AND INFORMATION TECHNOLOGY
INSTITUTE OF NUCLEAR AND PHYSICAL ENGINEERING

Mgr. Goran Bulatovič

Dissertation thesis resume

Analytical models and numerical simulations of quasi-one-dimensional heat transfer

To obtain the academic title of:	Philosophiae doctor, PhD.
In the doctorate degree study programme:	Physical engineering
In the field of study:	Electrical and electronics engineering
Form of study:	Full-time
Place and date:	Bratislava, March 2025

SLOVAK UNIVERSITY OF TECHNOLOGY IN BRATISLAVA
FACULTY OF ELECTRICAL ENGINEERING AND INFORMATION TECHNOLOGY
INSTITUTE OF NUCLEAR AND PHYSICAL ENGINEERING

Dissertation thesis has been prepared at: Slovak University of Technology in Bratislava
Faculty of Electrical Engineering and Information Technology
Institute of Nuclear and Physical Engineering
Ilkovičova 3, 841 04 Bratislava

Submitter: Mgr. Goran Bulatovič
Slovak University of Technology in Bratislava
Faculty of Electrical Engineering and Information Technology
Institute of Nuclear and Physical Engineering
Ilkovičova 3, 841 04 Bratislava

Supervisor: doc. Ing. Peter Bokes, PhD
Slovak University of Technology in Bratislava
Faculty of Electrical Engineering and Information Technology
Institute of Nuclear and Physical Engineering
Ilkovičova 3, 841 04 Bratislava

Readers: prof. RNDr. Igor Medveď, PhD
Czech Technical University in Prague
Faculty of Civil Engineering
Department of Materials Engineering and Chemistry
Thákurova 7, 160 00 Prague

Ing. František Világi, MSc., PhD
Slovak University of Technology in Bratislava
Faculty of Mechanical Engineering
Institute of Energy Machinery
Námestie slobody, 812 31 Bratislava

Dissertation thesis abstract was sent: .....

Dissertation thesis defence will be held on: ..... at .....
Slovak University of Technology in Bratislava
Faculty of Electrical Engineering and Information Technology
Institute of Nuclear and Physical Engineering
Ilkovičova 3, 841 04 Bratislava

prof. Ing. Vladimír Kutiš, PhD.
Dean of FEI STU

Abstract

The dissertation thesis focuses on researching, developing and applying analytical quasi-one-dimensional models to heat transfer by conduction and convection with primary application to oil-filled transformers. Key achievements include two analytical models. Firstly, an analytical model to conduction heat transfer with variable boundary conditions is developed for bodies of changing geometry. An application is made to transformer layered windings where the analytical model accounts for the presence of transformer partial cooling ducts while the winding multi-layer structure is represented by an anisotropic thermal conductivity. Also, an application is made to beams with uniformly increasing cross section where it is shown that the model can account for the beams uniformly increasing cross-sectional area. Secondly, a comprehensive analytical model for laminar flow in a vertically heated natural convection loop is developed for derivation of the equations for loop velocities and temperature distribution with inclusion of temperature-dependent dynamic viscosity. Both analytical models are verified by finite element and finite volume method simulations. The application to oil-filled transformers is also verified by experimental data.

keywords: quasi-one-dimensional, transformer winding, uniformly increasing cross section, natural convection loop, finite element method, finite volume method.

Contents

Introduction

Heat transfer occurs in three spatial directions, and to fully characterize it, we need to understand how heat moves along each of these axes. The traditional approach to solving heat transfer problems involves two primary methods: analytical and numerical. Analytical solutions provide exact mathematical expressions for temperature distributions or heat fluxes as functions of the spatial coordinates, such as x, y, and z. On the other hand, numerical solutions provide approximate

results, typically represented by a large set of discrete values. While numerical methods are universally applicable, analytical solutions are often reserved for simpler or symmetrical cases.

At first glance, one might argue that numerical solutions, which can be directly applied to complex geometries and boundary conditions, are sufficient. In fact, many times, this is the approach taken. However, relying solely on numerical simulations introduces several challenges:

1. Numerical calculations are inherently dependent on the discretization of the problem, and the accuracy of the solution is often sensitive to the resolution of the mesh and the numerical methods employed. Moreover, the results can sometimes be unreliable or prone to errors that may be difficult to identify without further validation from an analytical model or experiment.

2. Obtaining precise results from numerical simulations requires significant computational resources, particularly for complex 3D problems. This can lead to long processing times and a large consumption of computing power.

3. While numerical simulations offer numerical results, they do not provide the same intuitive understanding that analytical solutions do. For example, an analytical solution can clearly illustrate the relationships between material properties, geometric configurations, and temperature distribution, something that might require extensive and repeated simulations to reveal in a numerical approach.

These limitations underscore the importance of finding analytical solutions, which can then be validated and refined through numerical methods or experimental data. Likewise, an analytical model can serve as a confirmation of numerical simulations or experiments. The concept of quasi-one-dimensional (q1D) heat transfer offers an effective way to simplify complex 2D or 3D heat transfer problems by reducing them to 1D models through temperature averaging. This approach is particularly effective in cases when we are interested in investigating heat transfer in one particular direction or we need to know the value for average temperature.

1 Overview of quasi-1D models found in literature

This section provides a concise review of quasi-one-dimensional (quasi-1D) models found in literature. The primary objective is to identify techniques and approaches that could be instrumental in developing analytical quasi-1D models for heat transfer applications, particularly relevant to power transformers.

Quasi-1D model for straight fins

Cooling fins are designed to maximize heat transfer by convection through a high surface-to-volume ratio. Due to their geometry, heat flux is predominantly along the fin's height, but temperature variation is more significant along its length. The 2D heat conduction problem can be transformed into a quasi-1D model by averaging the cross-sectional temperature and analyzing how this averaged temperature varies along the fin's length. This approach [1] results in discrepancies of up to 4.7 %. when compared to a two-dimensional series solution, which is notably better than the standard one-dimensional approximation with errors up to 18.1 %. This highlights the effectiveness of quasi-1D approximations in capturing essential temperature variations while simplifying the computational complexity.

Quasi-1D approach to externally heated plates

In this inverse heat conduction problem, the goal is to deduce the time-varying surface heat flux from thermocouple measurements. The time-varying heat flux is replaced with zones of spatially constant heat flux corresponding to individual thermocouples [2]. The higher the number of zones, the better the approximation. Each zone is modeled as a 1D geometry, significantly simplifying the analysis. By solving the transient one-dimensional heat equation using Laplace transforms and incorporating thermocouple readings, a functional relationship for the surface zone flux is obtained. This method demonstrates how quasi-1D models can efficiently handle complex boundary conditions and temporal variations, providing valuable insights into the thermal behavior of the system while reducing computational complexity. The approach effectively decouples the spatial and temporal components of the prob-

lem, allowing for a more tractable solution without sacrificing significant accuracy.

Quasi-1D approach to calculating anisotropic thermal conductivity of metal heat spreader

In another study, a quasi-1D approach is applied twice to determine the anisotropic thermal conductivity of a metal heat spreader [3]. First, it is assumed that the temperature along the height of the spreader is averaged allowing for the examination of the temperature distribution along its radius. This leads to a modified Bessel equation, which can be solved analytically.

Secondly,a shape factor is introduced to modify the 1D approach into a quasi-1D approach, accounting for axial thermal resistance. The introduction of this shape factor involves numerical simulations and empirical data fitting to refine the model further. This iterative process enhances the accuracy of the computed radial and axial thermal conductivities. The method underscores the importance of incorporating geometric considerations and empirical validation to improve quasi-1D models' predictive capabilities.

Quasi-1D approach to curved surface longitudinal thermocouple

Quasi-1D heat transfer is developed for a medium with varying thickness, specifically within thermocouples used in micro nozzles. The model considers various energy conversion processes, including Peltier flux, heat conduction flux, convection through the inclined surface, Seebeck effect, and Joule heating [4]. By balancing these components, a differential equation is derived that describes the temperature distribution within the thermocouple pellet.

The study's strength lies in its ability to account for multiple heat transfer mechanisms within a single quasi-1D framework, significantly reducing computational demands compared to full 2D simulations. This highlights the efficiency and versatility of quasi-1D models when dealing with complex thermal systems.

Quasi-1D fluid flow due to changing cross-section area

The concept of quasi-1D flow is extended to fluid dynamics, where variations in cross-sectional area are considered [5]. Using control volume analysis and a staggered grid system, equations are developed that describe mass, momentum, and energy conservation within channels of variable cross-sections. This approach [6] allows for the modeling of flows in axisymmetric channels like convergent-divergent nozzles.

A staggered grid arrangement is used to numerically solve the varying cross-section channel equations for mass, momentum, and energy conservation. This approach effectively mitigate discretization errors, such as odd-even decoupling between pressure and velocity fields. The methodology showcases how quasi-1D approximations facilitate the analysis of intricate fluid dynamics problems while maintaining computational efficiency.

Natural convection in heated open-ended vertical channel

A quasi-1D model is applied to study natural convection in a heated vertical channel using density averaging and the Boussinesq approximation [7]. By formulating an equation for loop velocity, the quasi-1D model captures the essential physics driving the flow without resorting to more complex 3D models. This simplified approach provides valuable insights into the relationship between air speed, heat flux, and channel properties, demonstrating the utility of quasi-1D models in understanding natural convection phenomena.

Conclusion

In summary, the reviewed models illustrate the diverse applications and methodologies of quasi-1D models across various heat transfer and fluid dynamics problems. These models offer significant advantages in terms of computational efficiency and conceptual simplicity while retaining sufficient accuracy for many practical scenarios. Techniques such as cross-sectional temperature averaging, zonal approximations and control volume method enhance their applicability and precision. Overall, quasi-1D models represent a powerful toolset for tackling complex thermal and fluid systems.

2 Thesis aims

The aims of the thesis are:

1. Review 1D and quasi-1D heat transfer by conduction and convection models in literature and identify their similarities and differences. Verify models of quasi-1D heat transfer with FEM simulations that might be relevant for heat transfer in power transformers.

2. Simulate the heat conduction in power transformer windings with partial cooling ducts in order to verify a proposed analytical model and to obtain information that can be used to improve the cooling of the windings.

3. Formulate a general analytical model for quasi-1D heat conduction transfer for variable cross section and 1D curvilinear coordinate systems.

4. Develop a model for viscous natural convection heat transfer inside the power transformer partial cooling ducts and verify the model with FEM simulations and obtain information that can be used to improve the cooling of the transformer windings.

3 Methodology

The methodology presented in the dissertation thesis revolves around the development and application of a quasi-one-dimensional (q1D) analytical framework for modeling heat transfer, fluid flow, and temperature distribution in complex systems such as transformer windings and natural convection loops. The approach combines mathematical derivations, simplifications of multi-dimensional problems, and comparisons with numerical simulations such as FEM (finite element method) and FVM (finite volume method) and experimental data to validate the model's accuracy and applicability.

Quasi-one-dimensional modeling framework

The core of the methodology lies in the formulation of a quasi-one-dimensional model that reduces the complexity of three-dimensional heat transfer and fluid flow problems into a more manageable form.

This is achieved by averaging physical quantities, such as temperature, over specific cross-sections or dimensions while retaining essential dependencies on key spatial coordinates. For example, the averaged temperature $\bar{\theta}(x)$ is defined as an integral over a cross-sectional area, reducing the problem to a single coordinate (x) while accounting for variations in other directions through boundary conditions and effective parameters. The methodology is generalized to handle curved geometries such as polar coordinates, demonstrating its adaptability to different coordinate systems and configurations.

The q1D differential equation heat equation is derived using energy balance principles, where heat fluxes, convective boundary conditions, and internal heat generation are integrated over infinitesimal elements. The model incorporates thermal conductivity, convective heat transfer coefficients, and fluid velocity to describe heat transport within the system. This approach allows for the inclusion of anisotropic thermal properties and non-uniform boundary conditions, making it versatile for various geometries and applications.

Application to beams with uniformly increasing cross-section

Q1D approach is applied to analysis of the steady-state heat transfer in beams whose cross-sectional area increases uniformly along their length. The goal is to simplify the inherently two-dimensional heat transfer problem into a computationally efficient one-dimensional formulation while maintaining accuracy through comparisons with finite element method (FEM) simulations. The model considers beams with a geometry defined by an annular sector of finite thickness, characterized by convective heat transfer along the radial surfaces and prescribed temperatures at the curved boundaries. This kind of geometry and heat transfer has been considered by many authors, several examples can be found in [8], [9], [10], [11] and [12]. The q1D framework reduces the complexity of the problem by averaging temperature over the beam's cross-section. This reduction is achieved by transforming the governing two-dimensional heat equation into a one-dimensional form using proportionality coefficients k, which relate the surface temperature to the cross-sectionally averaged temperature. Then the q1D equations are solved with python and Wolfram Mathematica scripts. Finally, the accuracy of the q1D model is rigorously verified by comparing its predictions with FEM simulations.

Application to transformer windings

In the context of transformer windings, the q1D model is applied to analyze temperature distributions in foil-type windings with partial cooling ducts. The winding is divided into segments, each characterized by its heat transfer properties. The model accounts for radial and tangential heat conduction, as well as convective cooling at boundaries. By comparing the q1D results with FEM simulations and experimental data, the methodology demonstrates excellent agreement, validating its accuracy. The q1D model also provides insights into the impact of design parameters, such as insulation thickness and cooling duct placement, on temperature rise and heat dissipation efficiency.

Natural convection loops

For natural convection loops, the methodology extends the q1D framework to include fluid dynamics. The governing equations incorporate buoyancy-driven flow and energy transport within the loop. The model calculates average velocities and temperature rises in different sections (e.g., channel, fin, top, and bottom) and compares these predictions with FVM simulations. The results highlight the model's ability to capture key phenomena, such as velocity profiles and temperature gradients, with very good accuracy.

Validation and comparison

A significant aspect of the methodology is the verification of the q1D model against numerical simulations (FEM and FVM) and experimental data. Tables and figures in the thesis compare predicted values (e.g., temperature rise, velocity profiles) with simulation results and industrial test data. The q1D model outperforms simpler models, such as weighted average temperature and thermal resistance models, particularly in capturing tangential heat transfer and non-uniform temperature distributions.

Conclusion

The methodology in the thesis thesis presents a robust and versatile quasi-one-dimensional framework for analyzing heat transfer and fluid

flow in engineering systems. By combining analytical rigor, mathematical simplifications, and validation against numerical and experimental data, the model provides valuable insights into temperature distributions, heat dissipation, and fluid dynamics. Its application to transformer windings and natural convection loops highlights its practical relevance and potential for broader use in thermal management and design optimization.

4 Results: development and validation of our quasi-1D models

In this section we present the results of our research. First is presented the generalized quasi-one-dimensional model. The model then serves as a springboard for developing quasi-one-dimensional models for beams with increasing cross section, transformer windings and natural convection loops. These models are verified with FEM (finite element method) and FMV (finite volume method) simulations. The quasi-one-dimensional transformer winding model is also validated experimentally. We also present two formulas for an important parameter k - which relates the surface temperature to the cross-sectionally averaged temperature.

4.1 General formulation of our quasi-one-dimensional model

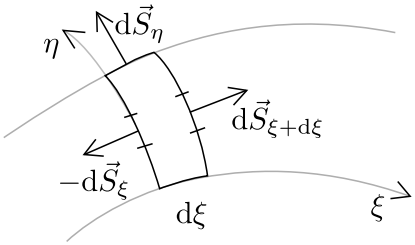

Figure 1: Two dimensional description of an infinitesimal element in orthogonal curved coordinates.

We seek an effective equation for the averaged temperature $\theta(\xi)$ which depends on a single curvilinear coordinate ξ - the direction the heat

transfer is being investigated in. The other two coordinates η, ζ define the cross-section of a heat-conducting solid, and averaging is performed over these coordinates:

$$\bar{\theta}(\xi) = \frac{1}{S_\xi} \oint_{S_\xi} \theta(\xi, \eta, \zeta) \mathrm{d}S_\xi \tag{4.1}$$

Assuming local orthogonality of coordinates and boundary surfaces defined by constant-coordinate planes, for clarity, the problem is considered in two dimensions (ξ, η) with all quantities uniform along ζ. The generalization to three dimensions follows similarly. The element in Fig. 1 is infinitesimal only along the coordinate ξ, along the coordinate η it extends over the whole cross section of the solid for $\eta \in (b_0, b_1)$. The steady-state energy balance for an infinitesimal element of area $\mathrm{d}S$ and volume $\mathrm{d}V$ gives:

$$\int_S \mathrm{d}\vec{S} \cdot \vec{q} = \int_V q_V \mathrm{d}V \tag{4.2}$$

where q is the heat flux density and q_V is heat generation per unit volume. Applying curvilinear coordinates, expanding terms via Taylor series, integrating over the element and using Fourier's law we obtain a generalized curvilinear differential equation

$$-\frac{\mathrm{d}}{\mathrm{d}\xi}\left[\int_{b_0}^{b_1} \lambda_\xi \frac{h_\eta}{h_\xi} \frac{\partial \theta(\xi, \eta)}{\partial \xi} \mathrm{d}\eta\right] + \sum_{\eta=b_0}^{b_1} \alpha_\eta \Big[\theta_\eta(\xi) - \theta_{\eta,\infty}(\xi)\Big] h_\xi = q_{c\mathrm{d}\xi} \tag{4.3}$$

where λ_ξ is thermal conductivity in the direction of ξ, index ∞ denotes fluid temperature sufficiently away from the solid's surface, α_η is the convective heat transfer coefficient, $\theta_\eta(\xi)$ is the convective surface temperature, h_ξ, h_η, h_ζ are Lame coefficients and $q_{c\mathrm{d}\xi}$ is the heat produced per $c\mathrm{d}\xi$

$$q_{c\mathrm{d}\xi} = \int_{b_0}^{b_1} q_V h_\xi h_\eta \mathrm{d}\eta. \tag{4.4}$$

Applying Eq. (4.1) to Eq. (4.3) cannot be done in a general way. Here we proceed to do it for Cartesian coordinates. Transforming Eq. (4.1) to a 2D Cartesian case we get

$$\bar{\theta}(x) = \frac{1}{b}\int_0^b \theta(x,y)\mathrm{d}y \tag{4.5}$$

which, with some manipulation, transforms Eq. (4.3) to

$$-\frac{\mathrm{d}}{\mathrm{d}x}\left[\lambda_x \frac{\mathrm{d}}{\mathrm{d}x}\bar{\theta}(x)\right] + \frac{1}{b}\sum_{y=0}^{b}\alpha_y\left[\theta_y(x) - \theta_{y,\infty}(x)\right] = q_V \tag{4.6}$$

when expressed in Cartesian coordinates. This equation has two variables: cross-sectionally averaged temperatures $\bar{\theta}(x)$ and surface temperature $\theta_y(x)$, y assuming either 0 or b. To have the equation closed we introduce an important parameter k - the coefficient of proportion between surface temperature rise and the cross-sectionally averaged temperature rise

$$\theta_y(x) - \theta_\infty = k_y(x)(\bar{\theta}(x) - \theta_\infty) \tag{4.7}$$

which changes Eq. (4.6) to

$$-\lambda_x \frac{\mathrm{d}^2\bar{\theta}(x)}{\mathrm{d}x^2} + \frac{2\alpha k(x)}{b}(\bar{\theta}(x) - \theta_{\mathrm{oil}}) = q_V \tag{4.8}$$

for the symmetric case when $k_0 = k_b = k$. Now the equation is purely one-dimensional. It can be shown that for the symmetric case

$$k(x) = \left(\frac{\alpha b(x)}{6\lambda_y} + 1\right)^{-1} \tag{4.9}$$

4.2 Application of our quasi-1D approach to beams with uniformly increasing cross section

We have a case of polar coordinates where the curvilinear coordinates transform as follows $\xi \to r, \eta \to \varphi$. The thermal conductivity may be assumed to depend on r only. This case represents a solid with uniformly increasing cross-sectional area, Fig. 2.

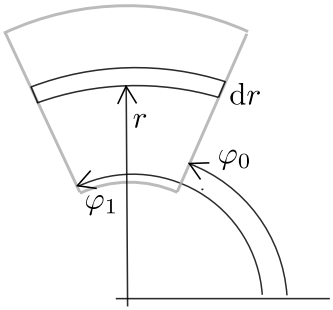

Figure 2: Polar coordinates in a curved solid (indicated by thick gray lines) with increasing cross-sectional area along the radial coordinate r. Also shown is the infinitesimal volume element for the the boundary surfaces characterized by φ_0, φ_1.

Now Eq. (4.3) takes form

$$-\frac{\mathrm{d}}{\mathrm{d}r}\left[r\frac{\mathrm{d}}{\mathrm{d}r}\bar{\theta}(r)\right]+\frac{2\alpha k(r)}{\lambda\Delta\varphi}\left[\bar{\theta}(r)-\theta_\infty\right]=\frac{q_V}{\lambda}r \tag{4.10}$$

where $\theta_\varphi(r)$ is the convective surface temperature at φ_0 or φ_1, $\Delta\varphi = \varphi_1-\varphi_0$ and the definition of the cross-sectionally averaged temperature is

$$\bar{\theta}(r)=\frac{1}{\Delta\varphi}\int_{\varphi_0}^{\varphi_1}\theta(r,\varphi)\mathrm{d}\varphi \tag{4.11}$$

and

$$\theta_\varphi(r)-\theta_\infty = k(r)[\bar{\theta}(r)-\theta_\infty] \tag{4.12}$$

Equation 4.10 describes the change of cross-sectionally averaged temperature $\bar{\theta}(r)$ in a a beam with uniformly increasing cross-section with two symmetric convective boundaries characterized by heat transfer coefficient α and fluid temperature θ_∞. We set two additional types of boundary conditions for the beam. The first type has zero flux for the non-convective boundary conditions and internal heat generation, Fig. 3 1). The second type has the two non-convective boundaries kept at temperatures θ_0 (at $r = r_0$) and θ_1 (at $r = r_1$) and there is no internal heat generation, Fig. 3 2).

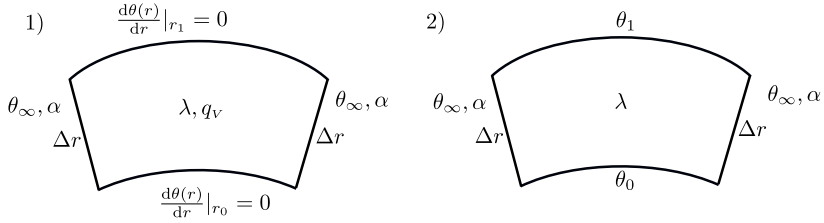

Figure 3: Both beams have two symmetric convective boundaries. The two non-convective boundaries are different. The first beam has internal heat generation, the second does not.

For the first type of the beam we transform Eq. (4.9) to polar coordinates

$$k(r) = \left(\frac{\alpha h(r)}{6\lambda} + 1 \right)^{-1} \tag{4.13}$$

where we substituted b with h for the cross sectional width. For the second type of beam we find a different formula for $k(r)$

$$k(r) = \frac{\sum_{n=1}^{N} E_n \sin(s_n r) + \theta_0 + \frac{\theta_1 - \theta_0}{L} r - \theta_\infty}{\sum_{n=1}^{N} \frac{2E_n}{h s_n} \sin(s_n r) \tanh(s_n h/2) + \theta_0 + \frac{\theta_1 - \theta_0}{L} r - \theta_\infty} \tag{4.14}$$

where

$$E_n = \frac{\frac{2\alpha}{L\lambda s_n}[\cos(s_n L)(\theta_1 - \theta_\mathrm{F}) - (\theta_0 - \theta_\mathrm{F})]}{s_n \tanh(s_n h/2) + \frac{\alpha}{\lambda}} \tag{4.15}$$

$$s_n = \frac{n\pi}{L} \tag{4.16}$$

Unfortunately, with the formulas for k, equation (4.10) cannot be solved analytically for either type of the beams. So we solve the quasi-1D equation numerically with Python and Wolfram Mathematica scripts to compare them with FEM simulations.

4.2.1 Comparison with FEM simulations

For both types of beams we choose $\alpha = 50$ W/(m^2·K), $r_0 = 1$ m, $r_1 = 2$ m. For the first type of beam we set $q_V = 50$ W · m^{-3}. For the second

type of beam we set the temperatures at $\theta_0 = 200\ ^\circ C$ and $\theta_1 = 100\ ^\circ C$. On the other hand, we choose three different values for the parameter $\Delta\phi = \pi/2$ (Fig. 4a), $2\pi/15$ (Fig. 4b) and $\pi/18$ (Fig. 4c) that represent three different geometries, and even larger set of thermal conductivities λ such that we explore three representative values of the Biot number

$$\mathrm{Bi} = \frac{\alpha \bar{h}}{2\lambda} \in \{0.5, 1, 10, 100\} \tag{4.17}$$

where $\bar{h}$ represents the beam medium width.

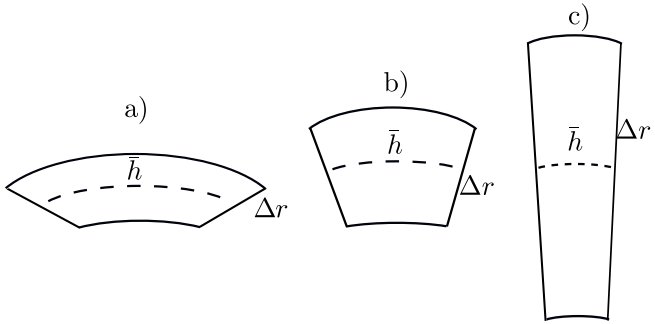

Figure 4: The three geometries tested: a) The mean width $\bar{h}$ is significantly bigger than the convective boundary Δr, b) $\bar{h}$ is approximately the same as Δr, c) $\bar{h}$ is significantly smaller than Δr.

The results show that, for both types of beams, FEM and model values for the cross sectionally averaged temperatures are in excellent agreement across a range of Biot numbers with largest discrepancy being just 1%. Even better, the discrepancy between FEM and the model for the average temperature rise $\Delta\bar{\theta}$ is less than 0.5 % for all tested Biot numbers. In essence, our quasi-1D analytical approach has succeeded in transforming the beams 2D temperature equation to 1D temperature equation, thus reducing the computational effort.

4.3 Application of our quasi-1D approach to transformer winding with partial cooling ducts

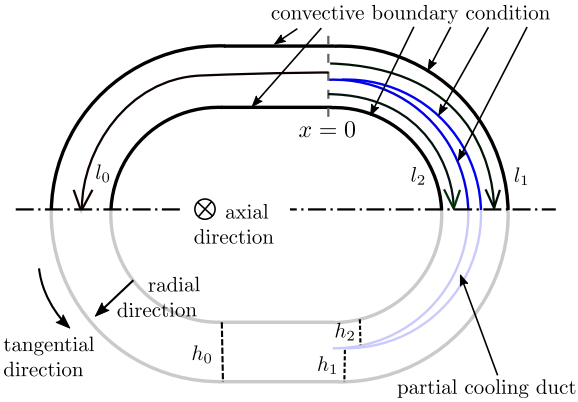

Figure 5: The winding is divided into segments and the cooling channels are represented by convective boundaries. Due to symmetry only the upper half of the winding needs to be considered. The three segments can be identified by their tangential lengths l_0, l_1 and l_2. The latter two are separated by a partial cooling duct.

The multilayer structure of the winding is replaced by a homogenous model with anisotropic thermal conductivity in the quasi-one-dimensional model

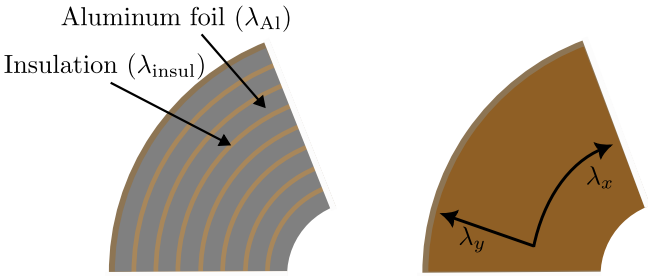

Figure 6: The multilayer structure of the foil winding (on the left) is replaced with a homogeneous model with anisotropic thermal conductivity (on the right).

so that the winding segment differential equation features thermal conductivity in the radial and tangential direction

$$-\lambda_x \frac{\mathrm{d}^2\bar{\theta}_i(x)}{\mathrm{d}x^2} + \frac{\kappa_i}{h_i}(\bar{\theta}_i(x) - \theta_{\mathrm{oil}}) = q_V, \quad i = 0, 1, 2 \tag{4.18}$$

where width b is replaced by the segment width h_i, x is a curvilinear coordinate, i is the segment number and the radial thermal conductivity λ_y is hidden in the formula for parameter κ. For symmetrical convective boundary conditions we have

$$\kappa_i = 2\alpha k_i, \quad k_i = \left(1 + \frac{\alpha h_i}{6\lambda_y}\right)^{-1} \tag{4.19}$$

and for two distinct heat transfer coefficients $\alpha_{0,i} \neq \alpha_{h,i}$,

$$\kappa_i = D_i^{-1}\left[\alpha_{0,i}\left(3/4 + 3f_{h,i}/2\right) + \alpha_{h,i}\left(3/4 + 3f_{0,i}/2\right)\right], \quad f_{0,i} = \frac{\alpha_{0,i}h}{4\lambda_y}, \quad f_{h,i} = \frac{\alpha_{h,i}h}{4\lambda_y} \tag{4.20}$$

The solution of Eq. 4.18 is

$$\bar{\theta}_i(x) = \theta_{\mathrm{oil}} + \gamma_i + B_i \cosh\left(\frac{x - l_i}{\delta_i}\right) \tag{4.21}$$

where

$$\gamma_i = \frac{h_i}{\kappa_i} q_V, \quad \delta_i = \sqrt{\frac{\lambda_x h_i}{\kappa_i}}, \quad B_i = C_i \frac{\frac{l_i}{\delta_i}}{\sinh\left(\frac{l_i}{\delta_i}\right)}, \tag{4.22}$$

and

$$C_i = \frac{\delta_i}{l_i} \tanh\left(\frac{l_i}{\delta_i}\right)\left[\gamma_0 - \gamma_i - \frac{\sum_{j=0}^{2} \frac{h_j}{\delta_j}(\gamma_0 - \gamma_j)\tanh\left(\frac{l_j}{\delta_j}\right)}{\sum_{j=0}^{2} \frac{h_j}{\delta_j}\tanh\left(\frac{l_j}{\delta_j}\right)}\right]. \tag{4.23}$$

Average winding temperature is given by

$$\bar{\theta} = \frac{\sum_{i=0}^{2} h_i l_i \bar{\theta}_i}{\sum_{i=0}^{2} h_i l_i} \tag{4.24}$$

where

$$\bar{\theta}_i = \frac{1}{l_i}\int_0^{l_i} \theta_i(x)\,\mathrm{d}x = \theta_{\mathrm{oil}} + \gamma_i + C_i. \tag{4.25}$$

4.3.1 Comparison with FEM simulations

We compare the analytical solution for $\bar{\theta}_i(x)$ with a two-dimensional FEM simulation of the low-voltage winding of a three phase transformer, label aTOHn 3710/22. In this transformer, both, low-voltage and high voltage winding have one partial duct. The temperature and heat flux along the axial direction is considered constant. The FEM 2D winding model is constructed in Gmsh [13] and the simulation is run in Elmer [14].

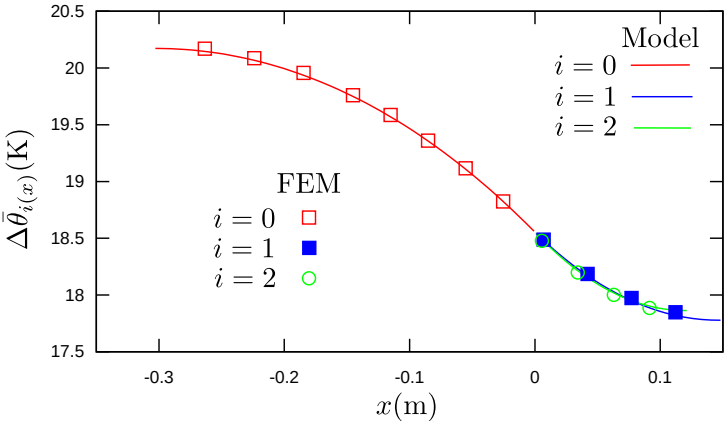

Figure 7: Comparison of the FEM and q1D model values for radially averaged temperature rise along the x axis over the three winding segments.

The agreement is excellent. Next, we compare the FEM simulation and model value for the low-voltage winding average temperature rise above the oil temperature $\Delta\bar{\theta}$. For an illustration, we add to the comparison values for $\Delta\bar{\theta}$ computed using lumped and slab model used in engineering for estimation of temperatures.

Table 1: Comparison of values for the winding temperature rise. Compared are the values obtained from the 2D FEM simulation with the values obtained from the q1D, weighted average and thermal resistance models.

model	FEM	q1D	slabs	lumped
$\Delta\bar{\theta}$ (K)	18.96	18.97	21.02	21.61
relative error from FEM (%)	n/a	0.0	10.9	14.0

Clearly, the q1D model provides the value closest to the FEM results. This is expected since the weighted average temperature (slab) and thermal resistance (lumped) models do not take into account the heat transfer in the winding tangential direction and their values are correspondingly higher.

4.3.2 Comparison with industrial data

Here we compare the quasi-1D model average temperature results with industrial test conducted by BEZ Transformatory, for both, low-voltage and high voltage winding, for transformer aTOHn 3710/22

Table 2: Comparison of industrial test values for average temperature rise with the q1D model values for transformer model aTOHn 3710/22. Due to the uncertainty of the partial cooling duct length, the values for the q1D model are expressed with a tolerance.

type of winding	Oil temp. $\bar{\theta}_{\text{oil}}$ (°C)	Indust. test $\Delta\bar{\theta}$ (K)	q1D model $\Delta\bar{\theta}$ (K)	Indust. test vs q1D model (%)
LV	36.8	18.80	18.97 ∓ 0.19	1 ∓ 0.9
HV	36.8	17.00	17.72 ± 0.24	4.2 ∓ 1.4

In the case of the low-voltage winding, for which the model is easier applicable, we get around 1 % discrepancy. In the case of the high-voltage winding, which is considerably more complex, we get around 4.2 % discrepancy with the industrial data. Thus the q1D model can be used effectively to predict the cooling power of a partial cooling duct added to an oil transformer winding [15].

4.4 Vertically heated natural convection loop model

In previous section we developed a quasi-one-dimensional framework to determine the temperature distribution within transformer windings. This approach, however, assumes temperature uniformity along the winding height, represented here by the z-axis. To extend this model and capture temperature variations with respect to height, we develop an analytical loop model specifically for transformer oil distribution.

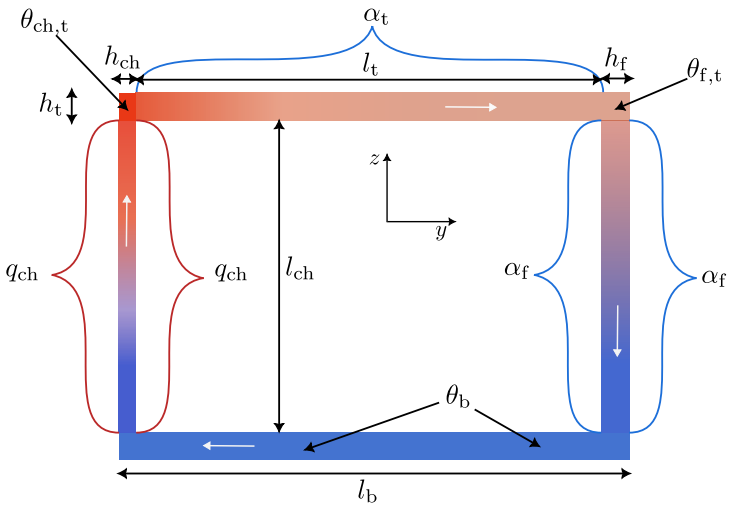

Figure 8: Model of a natural convection loop. On the left, the heat enters the channel from two walls characterized by q_{ch}. On the right, the heat leaves the fin through two walls characterized by α_{f}. On the top, the heat leaves the fin through one wall characterized by α_{t}

We have a natural convection loop that consists of a vertical channel and fin of length l_{ch} and widths h_{ch}, h_{f} respectively, horizontal top and bottom of width h_{t} and lengths $l_{\mathrm{t}}, l_{\mathrm{b}}$ respectively, Fig. 8. We consider that the loop has the same depth along the axis perpendicular to the fluid flow (x axis) and that there is no temperature and flux change along x axis. The loop is heated at the channel, with the heat amount characterized by surface heat flux density q_{ch}, and cooled at the fin and top, with the heat loss characterized by the fin and top heat transfer coefficients $\alpha_{\mathrm{f}}, \alpha_{\mathrm{t}}$. The rest of the loop - the bottom and loop two top corners - is considered insulated. The fluid is heated in the channel

to reach temperature $\theta_{\mathrm{ch,t}}$ which it retains in the left top corner of the loop. The fluid is then cooled in the top part of the loop to reach temperature $\theta_{\mathrm{f,t}}$ which it retains in the right top corner of the loop. The fluid is then cooled in the fin to reach temperature θ_{b}, which it retains in the bottom part of the loop. Using the q1D approach we obtain formulas for the loop fin, channel and top cross-sectionally averaged temperatures

$$\bar{\theta}_{\mathrm{f}}(z) = (\theta_{\mathrm{f,t}} - \theta_{\mathrm{a}})e^{c_{\mathrm{f}}(z-l_{\mathrm{ch}})} + \theta_{\mathrm{a}} \tag{4.26}$$

$$\bar{\theta}_{\mathrm{ch}}(z) = c_{\mathrm{ch}}z + \theta_{\mathrm{b}} \tag{4.27}$$

$$\bar{\theta}_{\mathrm{t}}(y) = (\theta_{\mathrm{f,t}} - \theta_{\mathrm{a}})e^{c_{\mathrm{t}}(l_{\mathrm{t}}-y)} + \theta_{\mathrm{a}} \tag{4.28}$$

where $\theta_{\mathrm{f,t}}$ is the value of the temperature for $z = l_{\mathrm{ch}}$, $k_{\mathrm{f}} = \left(1+\frac{\alpha_{\mathrm{f}}h_{\mathrm{f}}}{6\lambda}\right)^{-1}$, $k_t = \left(1 + \frac{\alpha_{\mathrm{t}}h_{\mathrm{t}}}{6\lambda}\right)^{-1}$, $c_{\mathrm{f}} = \frac{2k_{\mathrm{f}}\alpha_{\mathrm{f}}}{h_{\mathrm{f}}c_V\bar{\rho}\bar{v}_{\mathrm{f}}}$, $c_{\mathrm{ch}} = \frac{2q_{\mathrm{ch}}}{h_{\mathrm{ch}}c_V\bar{\rho}_{\mathrm{ch}}\bar{v}_{\mathrm{ch}}}$, and $c_{\mathrm{t}} = \frac{2k_{\mathrm{t}}\alpha_{\mathrm{t}}}{h_{\mathrm{t}}c_V\bar{\rho}\bar{v}_{\mathrm{t}}}$. For the bottom temperature we obtain

$$\theta_{\mathrm{b}} = (\theta_{\mathrm{f,t}} - \theta_{\mathrm{a}})e^{-c_{\mathrm{f}}l_{\mathrm{ch}}} + \theta_{\mathrm{a}} \tag{4.29}$$

We also obtain fin, channel and top average temperatures

$$\bar{\theta}_{\mathrm{f}} = \frac{(\theta_{\mathrm{f,t}} - \theta_{\mathrm{a}})\left(1 - e^{-c_{\mathrm{f}}l_{\mathrm{ch}}}\right)}{c_{\mathrm{f}}l_{\mathrm{ch}}} + \theta_{\mathrm{a}} \tag{4.30}$$

$$\bar{\theta}_{\mathrm{ch}} = \frac{c_{\mathrm{ch}}l_{\mathrm{ch}}}{2} + \theta_{\mathrm{b}} \tag{4.31}$$

$$\bar{\theta}_{\mathrm{t}} = \frac{(\theta_{\mathrm{f,t}} - \theta_{\mathrm{a}})\left(e^{c_{\mathrm{t}}l_{\mathrm{t}}} - 1\right)}{c_{\mathrm{t}}l_{\mathrm{t}}} + \theta_{\mathrm{a}} \tag{4.32}$$

To find loop velocities we formulate an integral equation for the force acting in the fluid on a volume V bounded by a closed surface S is given by mechanical stress and buoyancy force

$$\vec{F} \;=\; \oint \mathrm{d}\vec{S}\cdot \overleftrightarrow{\sigma} + \int \rho(\theta)\vec{g}\mathrm{d}V \tag{4.33}$$

where $\overleftrightarrow{\sigma}$ is the stress tensor and $\vec{g}$ is gravitational acceleration vector. We use a linear approximation for density change with temperature

$$\rho(\theta) = \rho_{\mathrm{ref}}(1 - \beta(\theta - \theta_{\mathrm{ref}})) \tag{4.34}$$

where β is the coefficient of thermal expansion and the reference density ρ_{ref} corresponds to the reference temperature θ_{ref}. We suppose that velocities are constant in the individual loop parts ($\vec{F} = 0$). Using velocity parabolic cross-sectional profile

$$v(y) = 4v_{\max}\left(1 - \frac{y}{h}\right)\frac{y}{h} \tag{4.35}$$

and continuity equation

$$\bar{v}_{\mathrm{f}} S_{\mathrm{f}} = \bar{v}_{\mathrm{ch}} S_{\mathrm{ch}} \tag{4.36}$$

we get

$$\bar{v}_{\mathrm{ch}} \quad = \quad \frac{g\rho_{\mathrm{ref}}\beta\left(\bar{\theta}_{\mathrm{ch}} - \bar{\theta}_{\mathrm{f}}\right)}{12\left(\frac{\bar{\eta}_{\mathrm{ch}}}{h_{\mathrm{ch}}^2} + \frac{\bar{\eta}_{\mathrm{f}} h_{\mathrm{ch}}}{h_{\mathrm{f}}^3}\right)} \tag{4.37}$$

for the channel cross-sectionally averaged velocity, where η is dynamic velocity. Other loop velocities are easily obtained with the continuity equation. We introduce an energy balance equation for the total heat amount entering the channel and exiting fin and top

$$q_{\mathrm{ch}} l_{\mathrm{ch}} = q_{\mathrm{f}} l_{\mathrm{ch}} + q_{\mathrm{t}} l_{\mathrm{t}} \tag{4.38}$$

Combining equations we arrive at the temperature

$$\theta_{\mathrm{f,t}} = \frac{q_{\mathrm{ch}} c_{\mathrm{f}} l_{\mathrm{ch}}}{\alpha_{\mathrm{f}} k_{\mathrm{f}} (e^{c_{\mathrm{t}} l_{\mathrm{t}}} - e^{-c_{\mathrm{f}} l_{\mathrm{ch}}})} + \theta_{\mathrm{a}} \tag{4.39}$$

Manipulating equations, we arrive at the channel velocity equation

$$\bar{v}_{\mathrm{ch}} - A\left[\frac{B\left(e^{\frac{C}{\bar{v}_{\mathrm{ch}}}} + 1\right)}{\bar{v}_{\mathrm{ch}}\left(e^{\frac{C}{\bar{v}_{\mathrm{ch}}}} - 1\right)} - \frac{\left(e^{\frac{D}{\bar{v}_{\mathrm{ch}}}} - 1\right)}{\left(e^{\frac{C}{\bar{v}_{\mathrm{ch}}}} - 1\right)}\right] \quad = \quad 0 \tag{4.40}$$

which contains only one unknown – the channel average velocity – and is only dependant on the loop geometric, material and flux parameters, where

$$A = \frac{g\rho_{\mathrm{ref}}\beta q_{\mathrm{ch}}}{12k_{\mathrm{f}}\alpha_{\mathrm{f}}\left(\frac{\bar{\eta}_{\mathrm{ch}}}{h_{\mathrm{ch}}^2} + \frac{\bar{\eta}_{\mathrm{f}}h_{\mathrm{ch}}}{h_{\mathrm{f}}^3}\right)} \tag{4.41}$$

$$B = \frac{k_{\mathrm{f}}\alpha_{\mathrm{f}}l_{\mathrm{ch}}}{h_{\mathrm{ch}}c_V\bar{\rho}} \tag{4.42}$$

$$C = 2B\left(1 + \frac{k_{\mathrm{t}}\alpha_{\mathrm{t}}l_{\mathrm{t}}}{k_{\mathrm{f}}\alpha_{\mathrm{f}}l_{\mathrm{ch}}}\right) \tag{4.43}$$

$$D = 2B \tag{4.44}$$

Note: In the model equations, the top of the loop is assumed to be cooled from both its upper and lower sides. However, in Fig. 8 and in the FVM simulations, cooling is applied only to the upper side. The reason for using symmetric cooling in the analytical model is the definition of the parameter k_{t}. The formula for k in in Eq. 4.7 was derived for a solid with thermal conduction and convective boundaries. In contrast, the top of the loop involves thermal conduction with convective boundaries plus a moving fluid. Despite this difference, the formula for k under symmetric boundary conditions provides a good approximation for both symmetric and asymmetric cooling at the loop top, as long as fluid flow is present in the loop. As a consequence, when modeling asymmetric cooling, the top heat transfer coefficient α_{t} in the analytical model must be set to half the value used in the FVM simulations.

4.4.1 Comparison with FVM simulations

We have two loop geometries which we label 1 and 2. The geometries are two-dimensional as we consider no velocity and temperature change along the x axis. Both geometries have common widths but different lengths, Tab. 3. All four FVM (finite volume method) simulations have common fluid parameters.

Table 3: Two loop geometries widths and lengths

	h_{ch}(mm)	h_{f}(mm)	h_{t}(mm)	l_{ch} (mm)	l_{t} (mm)
geometry 1	4.5	6	12	800	150
geometry 2	4.5	6	12	500	500

An additional common parameter is the ambient temperature θ_{a}= 16.5 °C. The heat transfer coefficients are different, are $\alpha_{\mathrm{f}} = 5$ W/(m^2·K), $\alpha_{\mathrm{t}} = 10$ W/(m^2·K). Please note that, while the fin has the heat transfer coefficient on both sides, the top has it only on the upper side, Fig. 8. We set two values for the channel heating, $q_{\mathrm{ch}} = 120\ \mathrm{W \cdot m^{-2}}$ which we label as A and $q_{\mathrm{ch}} = 180\ \mathrm{W \cdot m^{-2}}$ which we label as B. Two different geometries and two different channel heatings amount to four different setups: 1A, 1B, 2A and 2B. The simulations are done in Ansys Fluent [**Ansys**]. The type of simulation is viscous laminar flow, pseudo transient. The values we input into the analytical model are exactly the same as the values for the four FVM simulations with one exception, $\alpha_{\mathrm{t}} = 5$ W/(m^2·K), which is the half of the FVM simulation value, because we model the loop top in our analytical model as if it had two convective boundaries - unlike in Fig. 8.

Comparison of loop velocities and temperatures

The analytical model provides the average velocity in the direction of the flow which is responsible for increased heat transfer due to the fluid flow. This value is compared to FVM corresponding average velocity component in the direction of the flow which is z for the channel and fin and y for the top and bottom. FVM average velocity component values are extracted from simulations and model average velocity values are obtained from Eqs. (4.36) and (4.40). To solve Eq. (4.40) we write a script in Python which makes use of function fsolve. FVM average temperatures are extracted from simulations and model average temperature values are obtained from Eqs. (4.29), (4.30), (4.31) and (4.32). As an illustration, we compare the analytical model and FVM simulation results for the 2B setup, Tabs. 4 and 5. The quantities of interest are the channel and fin average velocities, and temperature rises above the ambient temperature.

Table 4: Comparison of the analytical model results with the FVM simulation for the channel and fin average velocities for the 2B setup. Velocity values include the standard deviation.

	Model (mm/s)	FVM (mm/s)	Relative difference (%)
$\bar{v}_{\mathrm{ch}}$	2.155	2.170 ± 0.018	0.69
$\bar{v}_{\mathrm{f}}$	1.616	1.628 ± 0.012	0.73

Table 5: Comparison of the analytical model results with the FVM simulation for the channel and fin average temperature rises for the 2B setup.

	Model (K)	FVM (K)	Relative difference (%)
$\Delta\theta_{\mathrm{ch}}$	19.57	19.84	1.37
$\Delta\theta_{\mathrm{f}}$	16.29	16.28	0.06

Next, we compare FVM and analytical model temperature change rise (above the ambient temperature) for the channel and fin. The FVM values are extracted from simulations and model values are calculated with Eqs. (4.26) and (4.27). Simulation 2B is chosen as a representative simulation.

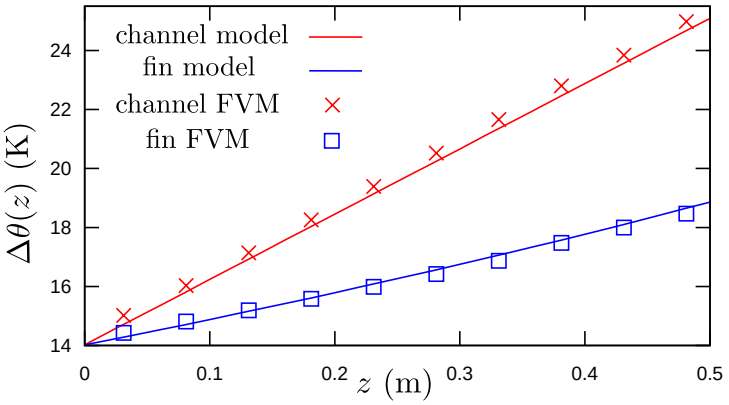

Figure 9: Comparison of the analytical model and FVM values for the temperature change (above the ambient temperature) in the channel and fin.

Overall, we get a very good agreement between the analytical model and the four FVM simulations for the loop velocities and temperatures. Almost all model values exhibit less than 2 % discrepancy with the FVM simulations.

5 Thesis conclusions

In this section, we examine the four objectives outlined at the beginning of the thesis.

1. We have reviewed a range of studies on 1D and quasi-1D heat transfer. A comparative analysis of these works is provided in the thesis introduction while individual reviews are found in the thesis first chapter. Our approach to quasi-1D heat transfer in transformer windings aligns most closely with the quasi-1D heat transfer approach to rectangular fins presented in [1], as elaborated in the thesis section on local ansatz for one-domesional slab.

2. We have simulated the heat conduction in power transformer windings with partial cooling ducts and have shown that the proposed analytical model offers valuable insights for improving the cooling efficiency of such windings. The model has no counterpart in literature and has been proven successful when compared with simulation and experimental data.

3. We have formulated a generalized analytical model for quasi-1D heat conduction in systems with variable cross section and applied it to beam with variable cross sections and oil-filled transformers. Three types of boundary conditions are explicitly treated in the model: zero flux, constant temperature and convective boundary characterized by heat transfer coefficient and fluid temperature. The model's accuracy has been validated against simulation data. Additionally, the model helped us develop the vertically heated natural convection loop model, which is discussed in the following objective.

4. We have developed a model for laminar viscous natural convection heat transfer within a vertically heated natural convection loop. This model serves as a foundation for analyzing natural convection in oil-filled transformers, with the ultimate goal of enabling

the prediction of axial temperature distributions and hot spots using purely analytical methods. The model has been proven successful when compared with simulation data. Furthermore, the natural convection loop model has broad applicability and can be adapted to various heating and cooling configurations, including side, vertical, and horizontal arrangements, to represent different technological applications driven by laminar natural convection. We also believe that the model can be extended to incorporate turbulent flow and non-uniform loop geometries, such as loops with varying heights. Upon successful expansion, the model could find applications in a diverse range of fields, including electronics cooling, solar water heating, emergency nuclear reactor cooling and geothermal reservoirs.

References

[1] A. Campo and A. Acosta-Iborra. "Corrected quasi one-dimensional heat conduction equation for the analysis of straight fins of uniform profile". In: *Heat and Mass Transfer* 55 (2019), pp. 1023–1031.

[2] H. Chen. "Two-Dimensional Formulation and Quasi-One-Dimensional Approximation to Inverse Heat Conduction by the Calibration Integral Equation Method". MA thesis. University of Tennessee, 2013.

[3] K. Mizuta et al. "Quasi one-dimensional approach to evaluate temperature dependent anisotropic thermal conductivity of a flat laminate vapor chamber". In: *Applied Thermal Engineering* 146 (2019), pp. 843–853.

[4] A. Hameed and R. Kafafy. "Thermoelectrically controlled micronozzle - A novel application for thermoelements". In: *Journal of Mechanical Science and Technology* 26.11 (2012).

[5] John D. Andersson. *Modern Compressible Flow*. 3rd revised. McGraw-Hill, 2003.

[6] Brett M Boylston. "Quasi-One-Dimensional Flow for Use in Real-Time Facility Simulation". MA thesis. University of Tennessee, Knoxville, 2011.

[7] V. Dubovsky. “Analytical study of natural convection in a heated vertical channel”. In: *HEFAT 2012 9th International Conference on Heat Transfer, Fluid Mechanics and Thermodynamics*. 2012, pp. 16–18.

[8] H. Liu et al. “Theoretical analysis of performance of variable cross-section thermoelectric generators: Effects of shape factor and thermal boundary conditions”. In: *Energy* 201 (2020).

[9] A. Hameed and R. Kafafy. “Uniform and Non-uniform Thermoelement Subject to Lateral Heat Convection”. In: *International Journal of Thermophysics* 34.3 (2013).

[10] S. Mahjoob and K. Vafai. “Analysis of Heat Transfer in Consecutive Variable Cross-Sectional Domains: Applications in Biological Media and Thermal Management”. In: *Journal of Heat Transfer* 133 (2011).

[11] B. Lu, X. Meng, and M. Zhu. “Numerical analysis for the heat transfer behavior of steel ladle as the thermoelectric waste-heat source”. In: *Catalysis Today* 318 (2018), pp. 180–190.

[12] A. Arenas, J. Vazquez, and R. Palacios. “Performance Analysis of Thermoelectric Pellets with Non-Constant Cross Sections”. In: *Material Science, Conference proceedings*. 2002.

[13] *Gmsh, a three-dimensional finite element mesh generator*. https://Gmsh.info/.

[14] *Elmer, an open-source Multiphysics simulation software*. http://www.elmerfem.org.

[15] G. Bulatovič and P. Bokes. “Impact of one and two partial cooling ducts on temperature rise in transformer windings”. In: *Journal of Physics: Conference Series* 2766 (2024).

List of author’s published articles

- G. Bulatović and P. Bokes, *Vertically heated natural convection loop model*, Journal of Electrical engineering, Vol. 5, (2024).
- G. Bulatovič and P. Bokes, *FEM verification of natural convection loop model*, Journal of Physics Conference Series Vol. 2911(1) (2024).

- G. Bulatovič and P. Bokes, *Impact of one and two partial cooling ducts on temperature rise in transformer windings*, ournal of Physics:Conference Series, Vol 2766 , (2024).

- M. Z. Diešková, S. Kotorová, G. Bulatović, and P. Bokes, *Simple model for heat transfer in magnetic nanofluid-enhanced oil-filled transformers*, AIP Conference Proceedings, Vol. 3251, (2024).

- S. Malinarič, P. Bokes and G. Bulatović, *New Numerically Improved Transient Technique for Measuring Thermal Properties of Anisotropic Materials*, Thermo, Vol. 4(3), (2024).

- P. Bokes and G. Bulatović, *Quasi-one-dimensional approach to heat transfer: general formulation and its application to transformer windings*, Applied Thermal Engineering, Vol. 248, (2023).

- G. Bulatovič and P. Bokes, *Quasi-one-dimensional treatment of heat transfer in beams of non-uniform cross-section*, Journal of Physics Conference Series Vol. 2628(1) (2023).

- G. Bulatovič and P. Bokes, *Numerical Evaluation of Anisotropic Thermal Conductivity Model of Foil Winding with Partial Cooling Duct*, AIP Conference Proceedings, Vol. 2801, (2023).

- G. Bulatovič and P. Bokes, *Limiting Behavior of Anisotropic Thermal Conductivity Model of Foil Winding with Partial Cooling Ducts*, Elitech Conference Proceedings, Vol. 24, (2022).